UNITED NATIONS UNIVERSITY
GEOTHERMAL TRAINING PROGRAMME
Orkustofnun, Grensásvegur 9,
IS-108 Reykjavík, Iceland

Reports 2010
Number 8

JOINT 1-D INVERSION OF TEM AND MT DATA – EXAMPLE FROM KRÝSUVÍK HIGH-TEMPERATURE AREA, SW-ICELAND

Boinaidi Ali Saïd
Ministry of Energy
B.P. 41 Moroni
COMOROS
boinaidalisaid@yahoo.fr

ABSTRACT

Krýsuvík is one of the high-temperature geothermal areas on the Reykjanes peninsula in SW- Iceland. In order to explore the geothermal potential of the area, 96 MT soundings were performed and more than 200 TEM soundings during the last few years. This report presents the results of a survey of one profile consisting of 10 MT soundings and 10 TEM soundings. Joint 1-D inversion of the TEM and MT data was done in order to correct the static shift affecting the MT soundings. The data were acquired by the geophysical team of ISOR for HS Orka and the data were processed, inverted and interpreted using different software like: SSMT2000, MTEditor, TEMX and TEMTD. The results of 1-D joint inversion given in this report are presented as cross-sections of the resistivity down to different depths. The 1-D inversion of TEM soundings reveals the subsurface resistivity down to a depth of less than 1 km, while the joint inversion of the TEM and the MT data reveals the subsurface resistivity down to a depth of several km. The geothermal reservoir is presumably located below 400 m b.s.l. according to the resistivity cross-section based on TEM soundings. The depth dimensions of the reservoir have been quite well defined by cross-sections based on MT soundings. Three favourable drilling locations are proposed to explore the geothermal resource.

1. INTRODUCTION

Magnetotellurics (MT) and Transient Electromagnetic (TEM) methods are widely used in geothermal exploration (Hersir and Björnsson, 1991). The magnetotelluric (MT) method is an important exploration technique for investigations of deep resistivity structures within the earth (Swift, 1967; Vozoff, 1991; Berdichevsky, 1999). Near-surface resistivity bodies can severely distort magnetotelluric (MT) apparent resistivity data at arbitrarily frequencies (Pellerin and Hohmann, 1990). This distortion, known as the MT static shift, is due to an electric field generated from boundary charges on near-surface resistivity inhomogeneities. TEM soundings are more correct in the subsurface since they do not measure the electric field, only the decay of the magnetic field. The overall objective of this report was to perform a joint 1-D inversion of TEM and MT soundings, using data from the Krýsuvík high-temperature area in SW-Iceland, to remedy the MT static shift.

Krýsuvík is one of the high-temperature geothermal areas on the Reykjanes peninsula in SW-Iceland. A total of 96 MT and more than 200 TEM sites have been acquired from the Krýsuvík high-temperature geothermal field and the surrounding area since 1989 and 1-D inverted (Eysteinsson, 1999

and 2001; Hersir et al., 2010). These data were used in this report with the permission of HS Orka to study the subsurface resistivity distribution of the Krýsuvík high-temperature geothermal field.

This report is divided into four parts. The first describes the generalities of the two methods used, MT and TEM. A discussion about the technical work, the data acquisition, how to record the data, process the data and make the joint inversion of the two data sets follows. The next step was to analyze the results from the joint inversion and interpret them to locate the geothermal reservoir area and identify favourable locations for geothermal exploratory drilling. Finally, conclusions and recommendations are presented.

2. RESISTIVITY METHODS IN GEOTHERMAL EXPLORATION

2.1 Transient electromagnetic method (TEM)

In TEM soundings, a magnetic field is artificially induced into the ground by a time varying (step) current transmitted into a loop or grounded dipole at the surface. Induction in a loop or potential difference is measured. Each time the transmitted current is abruptly turned off, an induced voltage is generated in the receiver (Figure 1). This induced transient voltage decays with time after the current switches. The induced voltage is measured in a receiver coil at the centre of a circular transmitter loop into which an alternating current, $I = I_0 e^{i\omega t}$, is transmitted. The induced voltage is given by:

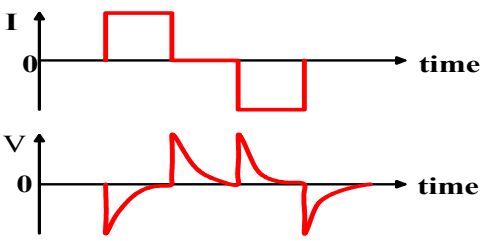

FIGURE 1: Transmitted current and transient voltage

$$V(\omega, r) = -i\omega\, \Phi(\omega, r)\, I_0 e^{i\omega t} \tag{1}$$

and

$$\Phi(\omega, r) = \int_0^\infty K(\omega, \lambda)\, J_1(\lambda r)\, d\lambda \tag{2}$$

where ω = The angular frequency;
K = The Kernel function;
I_0 = Current strength [A];
J_1 = The Bessel function of the first order; and
r = Radius of source loop [m].

The duration of each square pulse of the transmitted current is usually made long enough so that the transient voltage in the receiver has dropped to zero well before the current changes again.

The time domain response due to a sharp step function transmitted into the transmitter loop is calculated and given by the following formula (Árnason, 1989):

$$V_{step}(r, t) = \frac{2I_0}{\pi} \int_0^\infty Re\Phi(\omega, r) \cos(\omega t)\, d\omega \tag{3}$$

where I_o is the transmitted current strength; and
Φ is the Hankel transform integral for the frequency domain response.

The ramped step response is obtained by convolving the derivate of the current function with the sharp step response and the results in the integral are given as (Árnason, 1989):

$$V(r,t) = \frac{1}{TOFF} \int_{t}^{t+TOFF} V_{step}\Phi(r,\tau)\, d\tau \qquad (4)$$

where T_{OFF} = Turn-off time, the ramp length; and
τ = Time value.

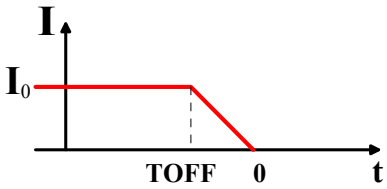

FIGURE 2: Ramped step function

The late time apparent resistivity values from the ramped step response (Figure 2) are a function of time after the current is turned off, given as (Árnason, 1989):

$$\rho_a(r,t) = \frac{\mu_0}{4\pi}\left|\frac{2\mu_0 I A_r n_r A_s n_s}{5t^{5/2}V(r,t)}\right|^{2/3} \qquad (5)$$

where μ_0 = Magnetic permeability in a vacuum [H/m];
A_r = Cross-sectional area of the receiver coil [m^2];
A_s = Cross-sectional area of the transmitter loop [m^2];
n_r = Number of windings in the receiver coil;
n_s = Number of windings in the transmitter loop;
V = The voltage response [V], the induced voltage at time t;
I = Current strength [A];
t = Time [s]; and
r = Radius of the transmitter loop [m].

The earth can be approached with an *N*-layered model (Figure 3). The depth of probing increases with time after the current is turned off.

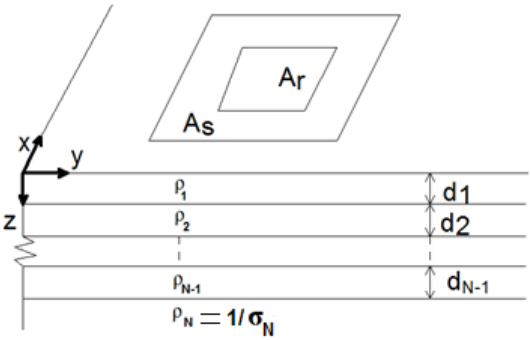

FIGURE 3: An N-layered half space model; the big square on the surface is the transmitter loop and the smaller one is the receiver coil; ρ_N = the resistivity of the Nth- layer; σ_N = the conductivity of the Nth-layer; and d_{N-1} = the thickness of the N-1-layer

In the central-loop TEM sounding, a *half-duty square wave* current is *transmitted* into a source loop. The *decay rate of the magnetic field* is measured, during *current off,* by recording the *induced voltage* in a *receiver* coil (antenna) at the centre of the source loop. The voltage is recorded at prefixed time gates, equally distributed in log-scale, as a function of time after current turn-off (see Figure 4).

The transmitter and receiver are synchronized, either by connecting them with a reference cable or by synchronized high precision crystal clocks, so that the receiver knows when the transmitter will turn off the current. It is impossible to turn off the current instantaneously (that would induce infinite voltage in the source loop). The transmitter is designed to turn off the current linearly from maximum to zero in a short but finite time called *turn-off time* (T_{OFF}). The zero time of the transients is the time when the current has reached zero; the time gates are located relative to this. This implies that the receiver has to know the turn-off time. The turn-off time is measured by the transmitter and fed by the operator into the receiver.

To reduce the influence of electro-magnetic noise, the recorded transients are stacked over a (user defined) number of cycles before being stored in the receiver memory. This is normally also done for different gains settings of the receiver. The depth of penetration of the sounding increases with time after the current turn-off. Different frequencies of the current signal are therefore used, high frequencies for shallow depths and low frequencies for deep probing (the time gates normally scale with the period T). Sometimes measurements are done with different antennas, e.g. a standard receiver coil, provided by the manufacturer, and larger effective area loops (induced voltage is dB/dt times the effective area of the antenna).

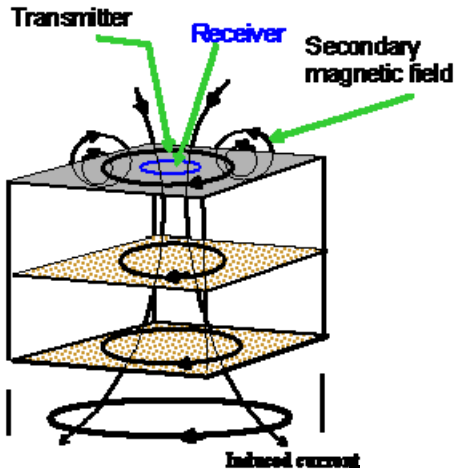

FIGURE 4: TEM sounding setup

2.2 Magnetotelluric method (MT)

The fluctuating natural electromagnetic field induces electrical currents in the conductive ground. By measuring the fluctuating magnetic field and the electrical currents (i.e. the electrical field) on the surface of the earth, it is possible to infer the resistivity of the earth below the measuring site.

The Magnetotelluric (MT) sounding method is based on measuring the currents induced in the ground by a time varying magnetic field, either the Earth's magnetic field or from currents transmitted into a grounded dipole on the surface. The induced currents are measured indirectly by measuring the voltage using two perpendicular dipoles on the surface; the source field is measured by magnetic induction coils parallel to the dipoles. MT is a powerful method used to probe deep resistivity structures. Using Maxwell's equations:

Faradays's law:

$$\nabla \times \boldsymbol{E} = -\mu \frac{\partial \boldsymbol{H}}{\partial t} \tag{6}$$

Ampere's law:

$$\nabla \times \boldsymbol{H} = \boldsymbol{J} + \varepsilon \frac{\partial \boldsymbol{E}}{\partial t} \tag{7}$$

while $\boldsymbol{J} = \sigma \boldsymbol{E}$
and $\rho = 1/\sigma$

where $\boldsymbol{E}$ = Electrical field intensity (V/m);
$\boldsymbol{H}$ = Magnetic field intensity (A/m);
$\boldsymbol{J}$ = Electrical current density (A/m^2);
σ = Electrical conductivity (S/m);
ε = Electrical permittivity (F/m); and
μ = Magnetic permeability (H/m).

In general, we have:

$\rho \approx 1 - 10^4$ Ωm
$\sigma \approx 1 - 10^{-4}$ S/m
$\omega = 2\pi/T$ and $T \approx 10^{-4} - 10^4$ s
$\varepsilon = \varepsilon_0 \chi_e$ and $\varepsilon_0 = 8.85 \times 10^{-12}$; and $\chi_e \approx 1 - 100$

or:

$k^2 = i\omega\mu(\sigma + i\omega\varepsilon) \cong i\omega\mu\sigma$ because $\sigma \gg \omega\varepsilon$ (quasi-stationary state).

For a homogenous earth (σ constant), it can be shown that:

$$H_x = \frac{-k}{i\omega\mu} E_y \tag{8}$$

$$H_y = \frac{k}{i\omega\mu} E_x \tag{9}$$

The impedance tensor (**Z**) describes the relationship between the electric and magnetic field. In matrix form this is given by:

$$\begin{pmatrix} E_x \\ E_y \end{pmatrix} = \begin{pmatrix} Z_{xx} & Z_{xy} \\ Z_{yx} & Z_{yy} \end{pmatrix} \begin{pmatrix} H_x \\ H_y \end{pmatrix} \tag{10}$$

or:

$$E_x = Z_{xx} H_x + Z_{xy} H_y \tag{11}$$

$$E_y = Z_{yx} H_x + Z_{yy} H_y \tag{12}$$

For layered (1-D) earth $Z_{xx} = Z_{yy} = 0$ and $Z_{xy} = -Z_{yx}$ which gives:

$$\vec{\boldsymbol{E}} = \begin{bmatrix} E_x \\ E_y \end{bmatrix} = \begin{bmatrix} 0 & Z_{xy} \\ Z_{yx} & 0 \end{bmatrix} \begin{bmatrix} H_x \\ H_y \end{bmatrix} = \overline{\boldsymbol{Z}}\vec{\boldsymbol{H}} \tag{13}$$

For a homogenous earth of resistivity (ρ) this means that:

$$Z_{xy} = \frac{E_x}{H_y} = \sqrt{\omega\mu\rho}\, e^{i\pi/4} \;\; or \;\; \theta_{xy} = \frac{\pi}{4} = 45°\,;\; phase\ difference, between\ E_x\ and\ H_y \tag{14}$$

$$\rho = \frac{1}{\omega\mu} |\boldsymbol{Z}|^2 = \frac{T}{2\pi\mu} \left|\frac{\boldsymbol{E}}{\boldsymbol{H}}\right|^2 \tag{15}$$

For an inhomogenous earth, we define the apparent resistivity (ρ_a) and phase (θ_a):

$$\rho_a = 0.2T|\boldsymbol{Z_0}|^2 \tag{16}$$

$$\theta_a = arg(\boldsymbol{Z_0}) \neq 45° \tag{17}$$

where Z_0 is the impedance on the surface $[(mV\ /\ Km)/nT]$.

The skin depth is defined as the depth where the electromagnetic field has reduced to e^{-1} of its original value at the surface. The skin depth is given as:

$$\delta = \frac{1}{Real(k)} = \frac{1}{Re\left(\sqrt{i\omega\mu\,\sigma}\right)} = \sqrt{\frac{2}{\omega\mu\,\sigma}} \tag{18}$$

or

$$\delta = 0.5\sqrt{\rho T}\ km \tag{18a}$$

3. TIMES SERIES ANALYSIS, INVERSION THEORY AND JOINT 1-D INVERSION

3.1 Digital recording

Waveforms are generally continuous functions of time or distance. To apply the power of digital computers in analysing the data, they need to be expressed in digital form, regardless of the form in which they were originally recorded. The digital recording allows replotting and processing of the data after recording. The recorder converts the input voltage into numbers and stores them.

Let the voltage output be *a(t)*. The recorder samples this function regularly in time, at a sampling interval Δt, and creates a sequence of numbers:

$$\{a_k = a\ (k\ \Delta t\ );\ k = 0,\ 1,\ 2,\ ...,\ N\ \} \tag{19}$$

The recorder stores the number as a string of bits in the same way as any computer.

Three quantities describe the limitations of the sensor: the *sensitivity* is the smallest signal that produces non-zero output; the *resolution* is the smallest change in the signal that produces non-zero output; and the *linearity* determines the extent to which the signal can be recovered from the output. For a digital recorder, linearity requires faithful conversion of the analogue voltage to a digital count, while resolution is set by the voltage corresponding to one digital count.

The recorder suffers two further limitations: the *dynamic range, g,* the ratio of maximum possible to minimum possible recorded signal, usually expressed in decibels: $20\ \log_{10}(g)$ dB; and the *maximum frequency* that can be recorded. For a digital recorder the dynamic range is set by the number of bits available to store each member of the time sequence, while the maximum frequency is set by the sampling interval Δt or *sampling frequency:*

$$v_s = 1/\Delta t \tag{20}$$

Normally the dynamic range, *g*, is a scale used to define electrical power ratios and it is an expression of the ratio of the largest measurable amplitude A_{max} to the smallest measurable amplitude A_{min} in a sampled function. The ratio of two power values P_1 and P_2 is given in decibels by:

$$10\log_{10}(P_1\ /P_2) =\ 10\log_{10}({A_{max}}^2)\ /\ ({A_{min}}^2) =\ 20\log_{10}(\mathrm{A_{max}}\ /\mathrm{A_{min}}) \tag{20a}$$

Storage capacity sets a limit to the dynamic range and sampling frequency. A larger dynamic range requires a larger number and more bits to be stored; a higher sampling frequency requires more numbers per second and, therefore, more numbers to be stored.

3.2 Processing

Data processing is about extracting a few nuggets from the dataset; it involves changing the original numbers, which always means losing information. So we always keep the original data. Processing involves operating on data in order to isolate a signal, the message that is interesting, and so separate it from noise, and unwanted signals. Processing is interactive and flexible; we are looking for something interesting in the data without being too sure of what might be there. A very important part of modern processing is the interaction between the interpreter and the computer.

The Fourier transform, in its various forms, decomposes a time series into its frequency components. In MT, raw time series are processed using calibration files, and site parameter files. The Fourier coefficients are calculated, which are then reprocessed with data from reference sites, using robust routines. And the output MT Plot file received contains multiple cross powers for each of the frequencies analyzed. Afterwards, the resistivity and phase curves are plotted, excluding noise. Then, there some parameters of the plot files which are displayed, such as tipper magnitude, coherency

between channels, and strike direction. Finally, the standard file is reached for the interchange of data from MT into what is called an Electrical Data Interchange (EDI) file.

3.2.1 Time series MT data

Suppose, having some data digitized as a sequence of N numbers:

$$\{a\} = a_0, a_1, a_2, ..., a_{N-1} \tag{21}$$

If the independent variable varies with time, the sequence is called a time sequence (or time series). In MT, 5 components (E_x, E_y, H_x, H_y and H_z) are measured.

There are no standard units for time series data because the system depends on the nature of data acquisition. Generally, units are integers representing raw data before system response has been removed. At this level, one needs a good knowledge of the response of the measurement and recording system used for acquiring the data. Because of the tremendous data volume, and its system dependent nature, time series data are not usually included with delivered data. It is only delivered when special reprocessing requirements preclude the use of another form of the data such as power spectra. Figures 5 and 6 give examples of MT data, time series of E_x and H_y (Figure 5), and E_y and H_x (Figure 6).

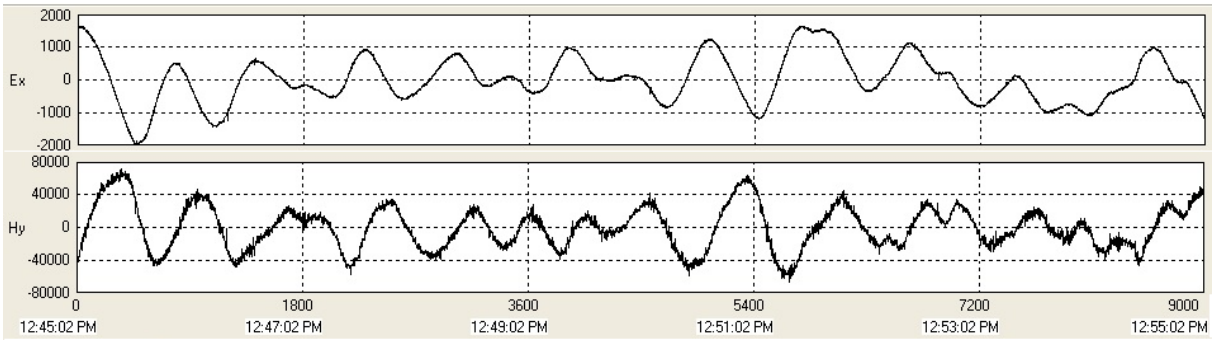

FIGURE 5: MT data, E_x and H_y as a function of time

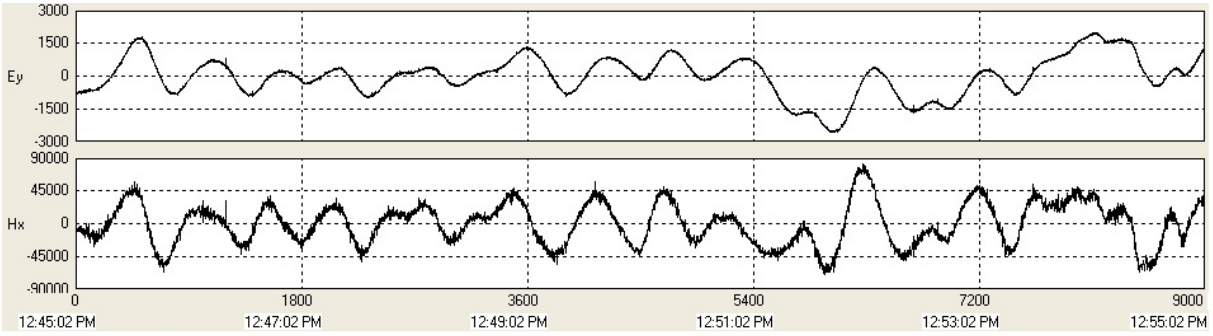

FIGURE 6: MT data, E_y and H_x as a function of time

On these two figures of time sequence, the auto correlation and cross correlation between E_x and H_y, and E_y and H_x is analyzed. Suppose the sequence $\{e_k;\ k = 0, 1, 2, \ldots, N-1\}$ is the time sequence obtained in the component E_x and the sequence $\{h_l;\ l = 0, 1, 2, \ldots, M-1\}$ is the time sequence given by the component H_y. The cross correlation of a time sequence with itself, the time sequence e, is called the auto correlation and is given as:

$$\phi_p = \frac{1}{N}\sum_k e_k e_{k+p} \tag{22}$$

And the cross correlation of two time sequences e and h is defined as:

$$c_p = \frac{1}{\mathrm{N}} \sum_k \mathrm{e}_k h_{k+p} \tag{23}$$

where p is called the lag, and N and M are the lengths of e and h, respectively.

Now consider the correlation in the frequency domain, the Discrete Fourier Transform of the auto correlation, the power spectrum:

$$\Phi_n = |E_n|^2 \tag{24}$$

$|E_n|$ is the amplitude spectra of the time sequence e for E channel.

3.2.2 Power spectra

$$|E_n|^2 = \frac{1}{N^2} \sum_{k=0}^{N-1} \mathrm{e}_k \, e^{-2\pi i n k/N} \sum_{l=0}^{N-1} \mathrm{e}_l \, e^{+2\pi i n l/N} \tag{25}$$

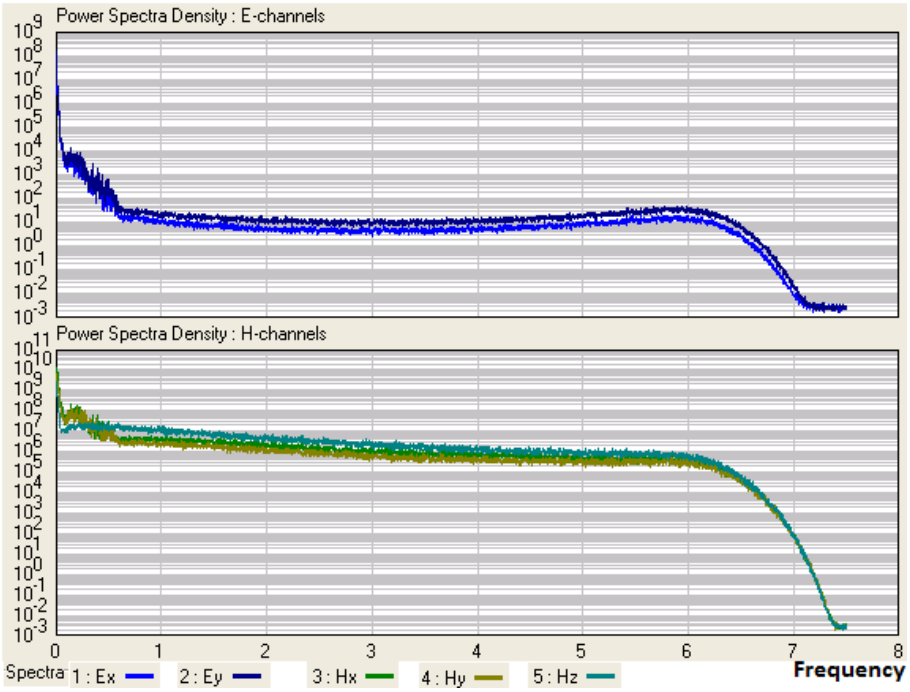

FIGURE 7: Power spectra

Stacked spectra (Figure 7) are a good way to deliver "raw" data which may be reprocessed at a later stage using alternate processing algorithms. Even if computed parameters are delivered, it may be a good idea to also deliver spectra. Because stacked spectra are a compact representation of the "raw" data, they are often the preferred way of delivering unprocessed data.

It may be desirable to also have the individual spectra segments prior to stacking. This allows re-stacking of the data at a later time, perhaps resulting in higher data quality. If spectra segments are delivered, it is recommended that they be in addition to the final stacked spectra and that they be delivered in a separate EDI file.

3.2.3 Signal amplitude and coherencies

Figure 8 shows the variation of the coherency of the electric and magnetic field as a function of the frequency. The vertical axis represents the coherency and the x-axis represents frequency. The blue curve shows the variation in the coherency of E_x and H_y over the frequency measured, while the green curve shows the variation in the coherency of E_y and H_x compared to the frequency measured.

3.3 Inversion

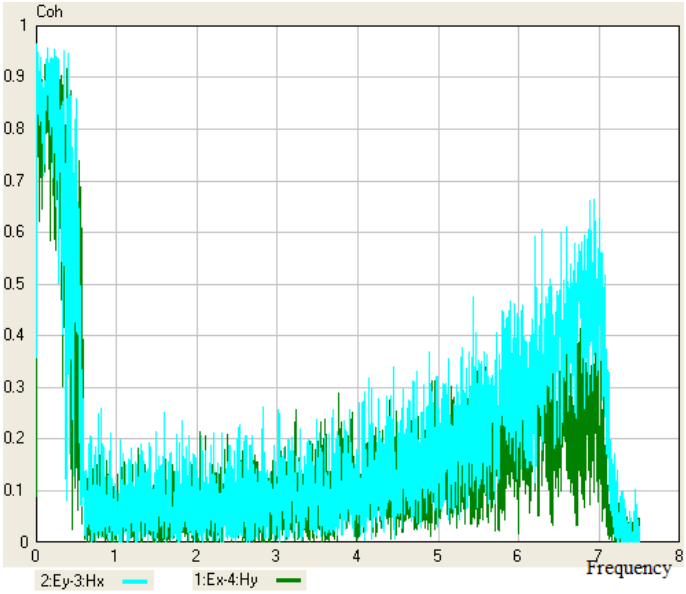

FIGURE 8: Coherency of *E* and *H*

The processed data are rarely the final end product; some further interpretation or calculation is needed. Usually it is needed to convert the processed data into other quantities more closely related to the physical properties of the target. In our case, the electromagnetic response of the layered earth is measured in order to determine the resistivity structure of the subsurface. In order to do that, two problems must be solved: *the forward problem* and the *inverse problem*.

In transient electromagnetic soundings, the earth is excited using the transmitter and we want to determine the resistivity structure of the subsurface from the measured response in a receiver, and then interpret the resistivity in the context of a geothermal reservoir.

Inversion is a way of transforming the data into more easily interpretable physical quantities. Forward modelling involves using the laws of physics to predict the observations from a model. A large set of models can be searched to find the one that fits the data. An example of the processing of TEM data is shown in Figure 9, showing the data and calculated response after 5 iterations using inversion.

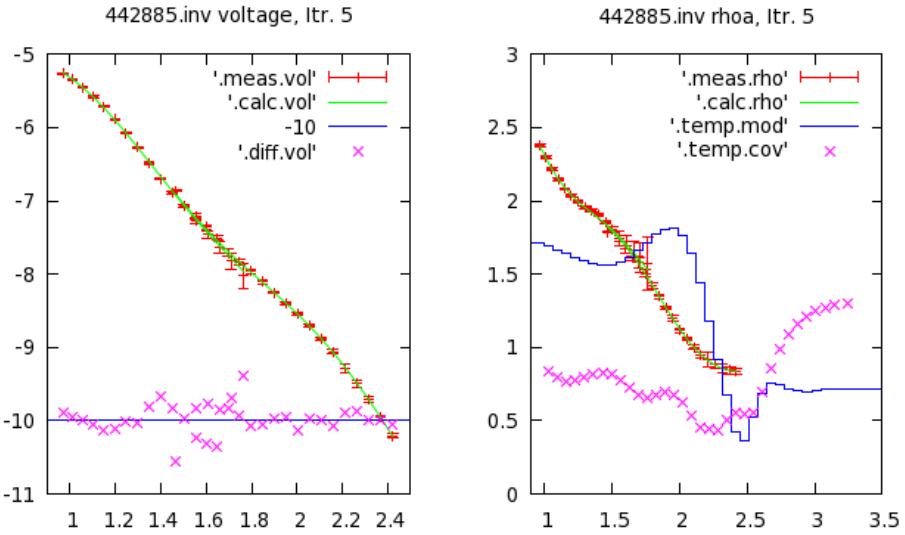

FIGURE 9: Processing of collected data from a TEM sounding showing the status of interpretation of the sounding during inversion after 5 iterations

There are two separate problems, existence and uniqueness. The first requirement is to find one model, any model, which fits the data. If none is found, the data are incompatible with the model. This is rare. Either there is something wrong with the model or the accuracy of the data has been overestimated. Having found one model, we search for others. If other models are found the solution is non-unique; account must be taken of it in any further interpretation. This always happens. The non-uniqueness is described by the subset of models that fits the data.

It is more efficient, when possible, to solve directly for the model from the data. This is not just an exercise in solving the equations relating the data to the model for model solution, the non-uniqueness must also be characterised by finding the complete set of compatible solutions and place probabilities on the correctness of each individual model.

There are two sources of error that contribute to the final solution, one arising because the original measurements contain errors, and one arising because the measurements failed to sample some part of the model. The largest source of error in the model usually comes from failure to obtain enough of the right sort of data, rather than sufficiently accurate data.

4. TEM AND MT MEASUREMENTS IN THE KRÝSUVÍK HIGH-TEMPERATURE AREA

4.1 The Krýsuvík area and the location of the TEM and MT measurements

The main aim of this report was to learn about the application of MT and TEM measurements. Data from the Krýsuvík high-temperature geothermal field were used for that purpose. The location of TEM and MT soundings in Krýsuvík used in this report and the associated resistivity profile are given in Figure 10. The data were measured and 1-D interpreted by ISOR's staff for HS Orka (Hersir et al., 2010), and are used here with their permission. Ten MT soundings and ten TEM soundings belong to this NW-SE cross-section. The MT soundings are shown with black dots and numbers as their names, while the TEM soundings are shown as green diamonds (Figure 10).

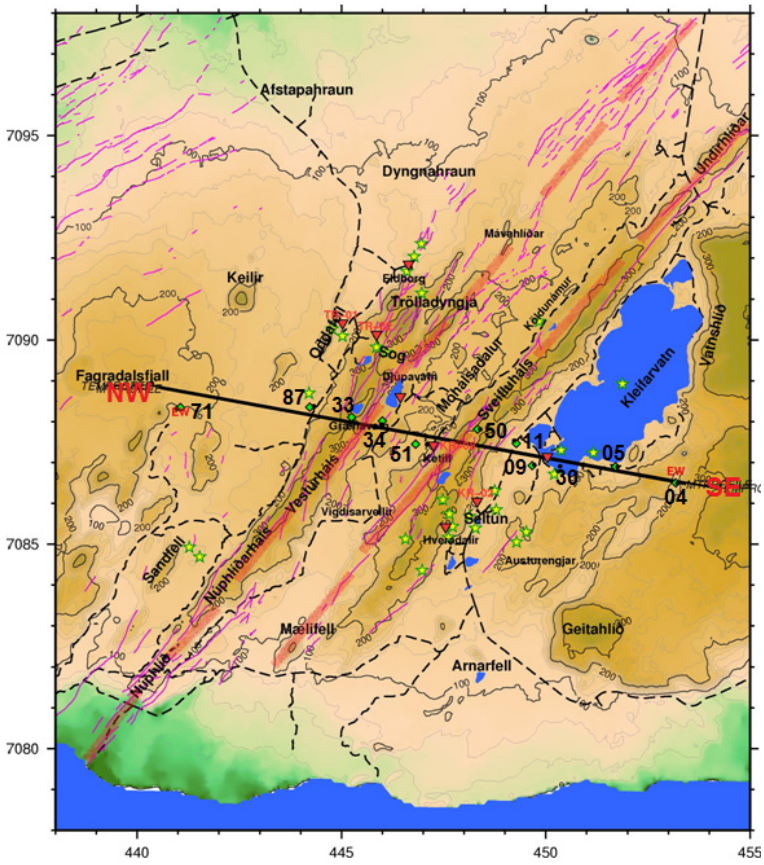

FIGURE 10: Location of TEM soundings (diamonds) and MT stations (dots), the resistivity profile, drillholes (inverted triangles) and surface manifestations (stars) and faults and fissures

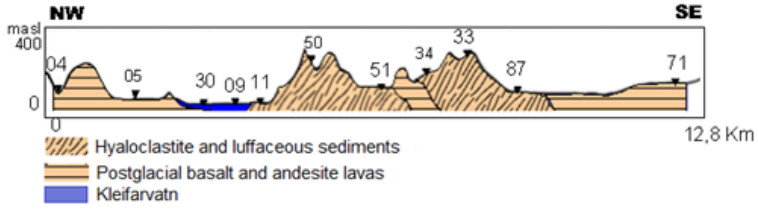

FIGURE 11: Surface geology

4.2 Measuring instruments

The TEM instruments used are from Geonics Ltd. in Canada. The soundings from TEM can reveal the subsurface resistivity down to a depth of about 0.5-1 km, depending on the resistivity distribution of the area. For low subsurface resistivity, the depth of penetration can be as low as a few hundred metres; but in higher resistivity surroundings, it is possible to explore the resistivity down to about 1 km. The MT instruments used in Krýsuvík are from Phoenix Ltd. in Canada (MTU type) (Figure 12).

4.3 Processing of the data

All the TEM data was interpreted in terms of 1-D inversion (resistivity only varies with depth) using the TEMTD program developed by ISOR – Iceland GeoSurvey (Árnason, 2006). Figure 13 shows an example of a sounding (TEM 49587) plotted on a log-log scale, with the measured (red stars) and calculated resistivity (black line) shown as a function of the square root of time after turn off, while the interpreted resistivity model (green curve) is plotted as a function of depth.

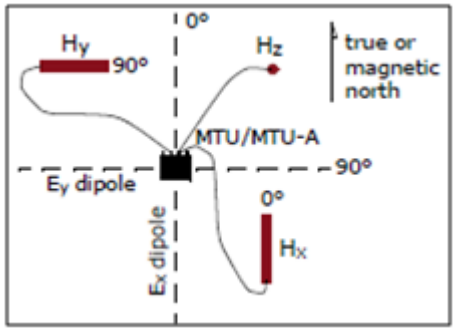

FIGURE 12: MT sounding setup (Phoenix Geophysics, 2009)

The big problem with MT soundings is their vulnerability to static shift, where the apparent resistivity curve can shift up or down and thus distort the results. TEM soundings are not affected by this and, thus, to counteract the static shift problem of the MT soundings, TEM data from the same site were used and jointly inverted with MT data in the 1-D inversion of the rotationally invariant determinant of the impedance tensor. The MT apparent resistivity must be divided by the shift multiplier in order to get the shift corrected apparent resistivity to tie in with the TEM data. Figure 14 shows an example of such a joint inversion (TEM 49587 + MT30). Appendix I shows the TEM and MT soundings that were jointly inverted, both data and interpretation.

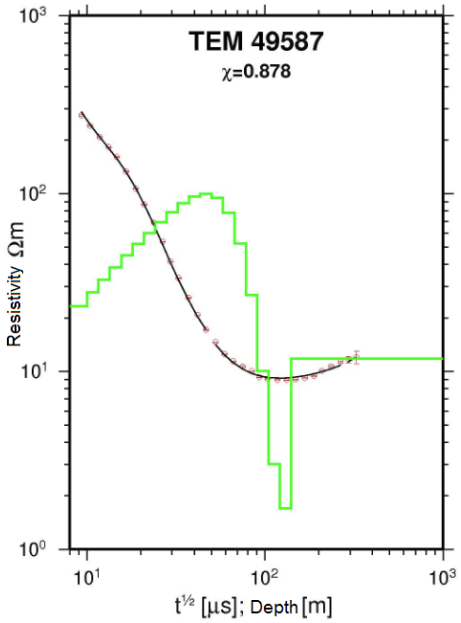

FIGURE 13: 1-D inversion of a TEM sounding TEM 49587

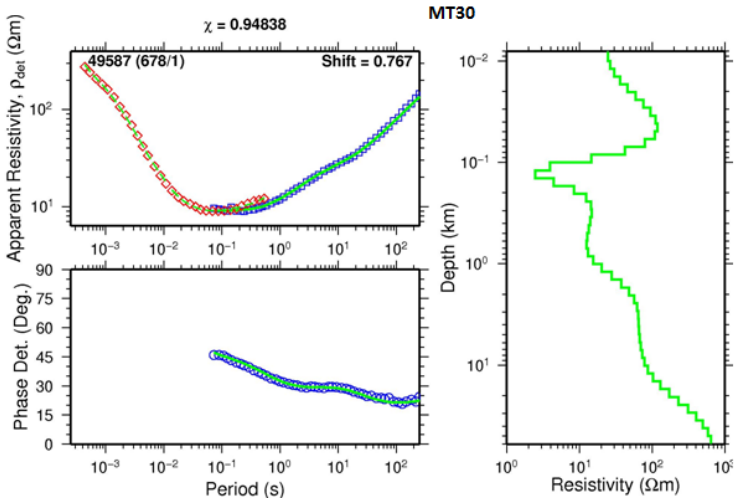

FIGURE 14: Results of joint 1-D inversion of TEM sounding 49587 and MT sounding MT30 in Krýsuvík, with measured apparent resistivity and phase curves, and the resulting resistivity model

5. INTERPRETATION AND RESULTS

The main aim of the project was to learn how to analyze and interpret the resistivity data using joint 1-D inversion, to interpret how it is possible to characterise the geothermal reservoir based on this data, and to locate favourable sites for drilling. Figure 15 shows the resistivity cross-section based on the results of the interpretation of the TEM measurements. Also shown are alteration zones found in well KR-8 (Arnórsson et al., 1975), which is located close to the cross-section. The resistivity cross-section shows, in general, two main resistivity structures:

- Between *320 and 0 m a.s.l.,* high-resistivity surface layers (>100 Ωm) are dominant and can be interpreted as unaltered basaltic lavas and hyaloclastites;

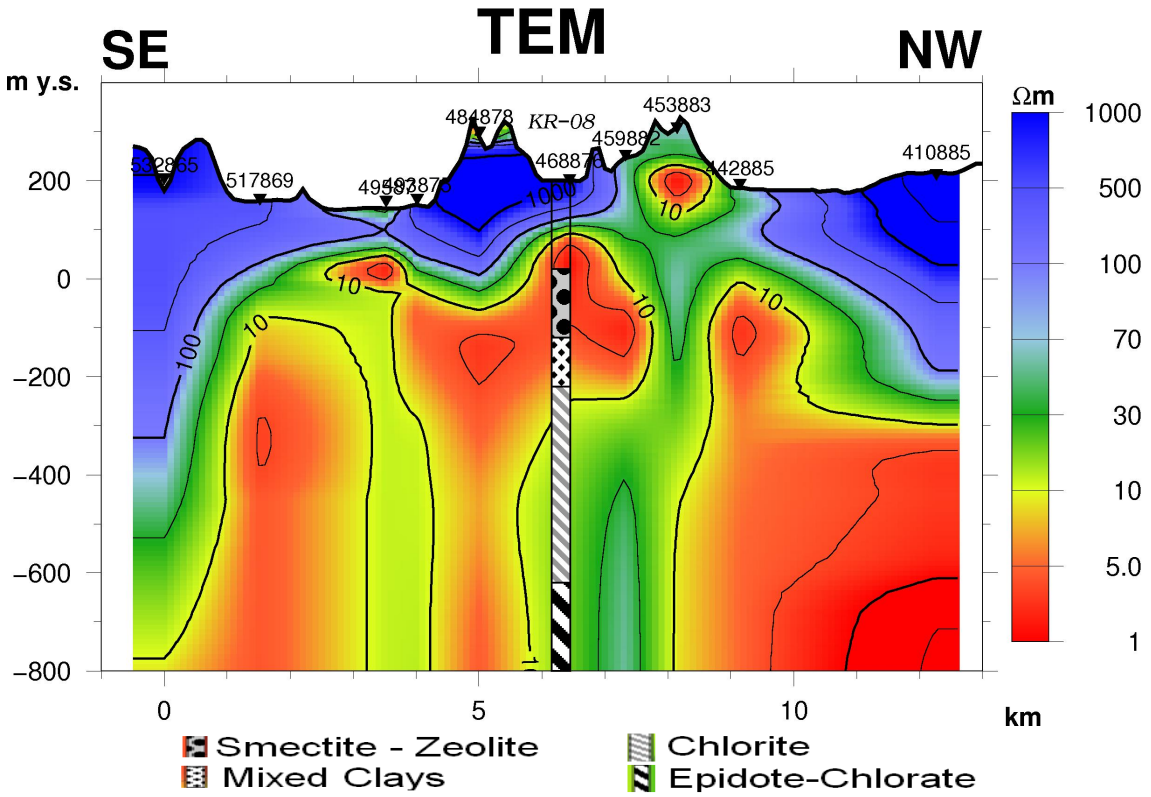

FIGURE 15: Resistivity cross-section from the 1-D inversion of TEM soundings, extending down to 800 m b.s.l.

- While between *0 and 800 m b.s.l.,* a low resistivity layer (≤ 10 Ωm), below the high-resistivity layers, can be correlated with the smectite-zeolite or mixed layer clay alteration zone, indicating geothermal activity.

Below the conductive layer, slightly higher resistivity (> 10 Ωm) is observed, which then can be correlated to the chlorite-epidote alteration zone seen in well KR-08 to a depth of about 933 m.

Figure 16 and the following figures are based on the joint inversion of TEM and MT data; now the

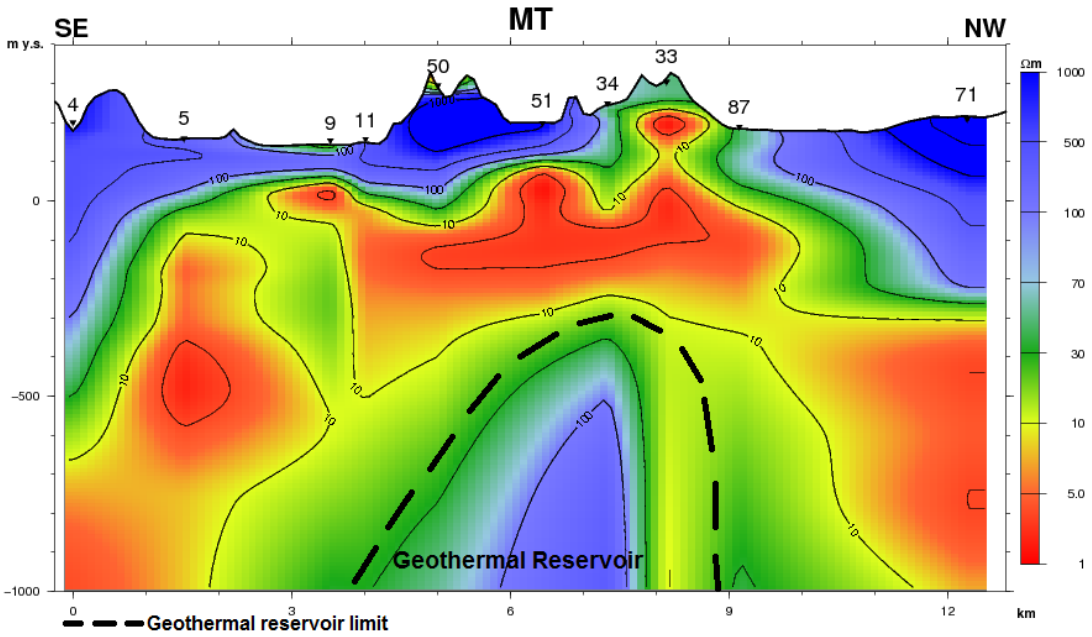

FIGURE 16: Resistivity cross-section based on joint 1-D inversion of TEM and MT data, extending to 1 km b.s.l.

results are far deeper reaching. In Figure 16, the resistivity is shown down to 1 km b.s.l. Here the cross-section allows distinguishing clearly between the upper conductive layer, which can be interpreted as geological formations with alteration indicating temperatures below about 220°C, and a more resistive layer below the central part of the geothermal area, which is probably the main geothermal reservoir. The figure also allows presuming the location of the top of the geothermal reservoir to be at about 300 m b.s.l. between MT soundings 51 and 33.

Following Figure 16, by analyzing the topography of MT sounding 33, it seems possible that the survey was implemented on a fissure. Under sounding 33, there is conductive zone reaching down to 1 km depth by an extension to the west and east of the profile studied. Following the structural analysis of the resistivity in Figure 16, the outcrops existing between soundings 34, 33 and 87 represent the conductive layer (usually seen at deeper levels) which represents altered rocks, based on temperature in the interval 100-220°C. The geological formations are hyaloclastites and tuffaceous sediments.

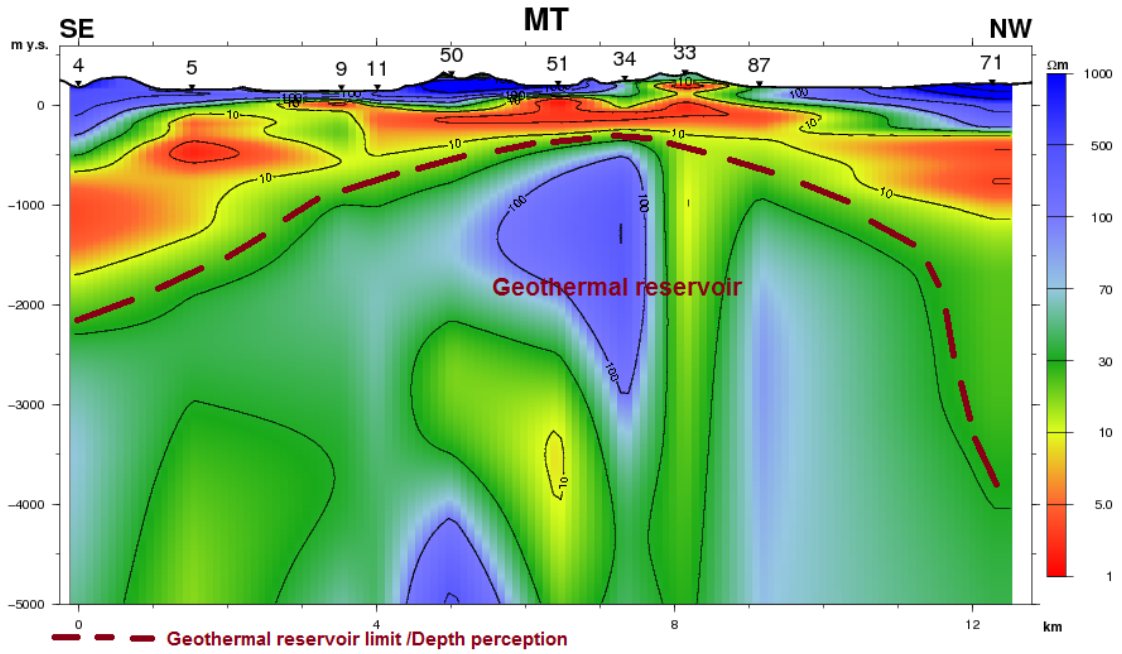

FIGURE 17: Resistivity cross-section from the joint 1-D inversion of TEM and MT extending down to 5 km b.s.l.

Figure 17 shows the variation of resistivity down to a depth of 5 km b.s.l., while Figure 18 stretches down to 10 km b.s.l. These cross-sections allow some determination of the dimensions of a reservoir with depth. The main reservoir seems to be located below MT soundings 50 and 33, about 4 km wide.

In Figure 18 it is complex to determine the geothermal heat source. We need other MT and TEM profiles to characterise and to determine the geothermal heat source that feeds this area.
Figure 19 shows the resistivity down to 2.5 km b.s.l., with proposed sites for drilling. Analyzing Figure19 according to the resistivity of the rocks, it can be noted that southeast of the profile, between MT soundings 5 and 9 from 0 to 700 m depth there is a conductive structure between the altered formations that may well be a promoter for geothermal exploitation.

So below MT sounding 9, a little west of the profile, close to Lake Kleifarvatn (see Figure 6) from 0 to 1.2 km deep, a favourable place for exploitation of the geothermal potential of this area is suggested. This favourable place can also be seen very well in Figure 15 under TEM sounding 49587. The proposed drill site is presented as a black bar in Figure 19.

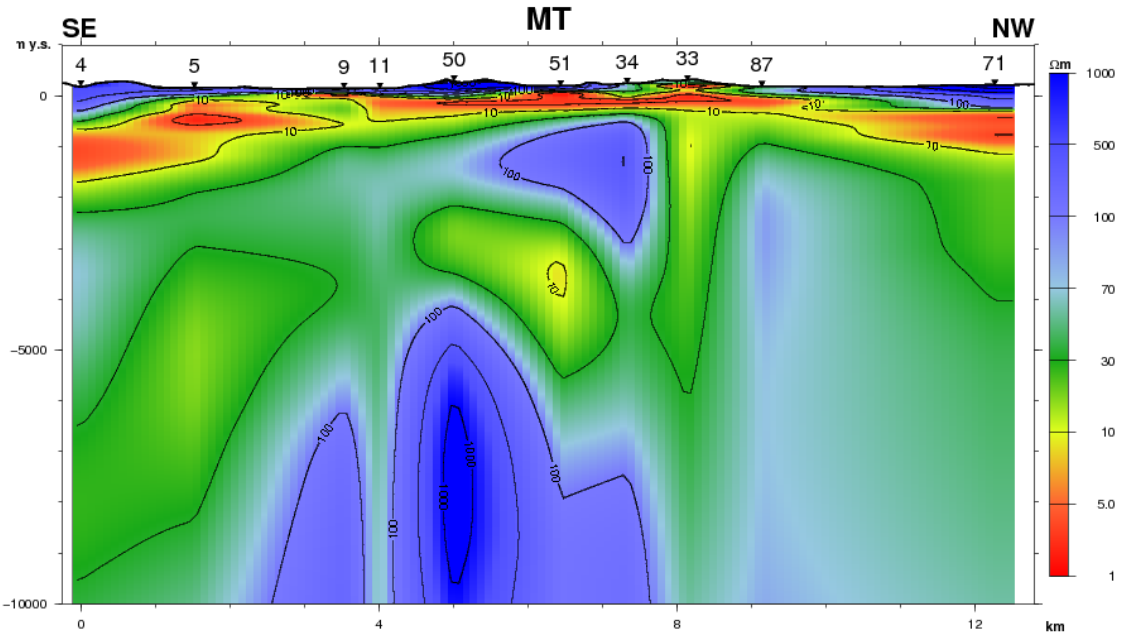

FIGURE 18: Resistivity cross-section from the joint 1-D inversion of TEM and MT extending down to 10 km b.s.l.

At the centre of the profile, between soundings 51 and 34, from 0 to 1.7 km depth, a second favourable place for exploitation is located. The surface geological formations dominant in this area are postglacial basalt and andesite lavas (see Figure 7). The proposed drill site is presented as a black bar in Figure 19.

To the northwest on the profile, just west of MT sounding 87, a third place for implementation is localized, from 0 to 1.3 km depth. But as there is a long distance between MT soundings 87 and 71 without data, it is recommended that additional soundings are conducted in this area in order to achieve better information. The proposed drill site is presented as a black bar in Figure 19.

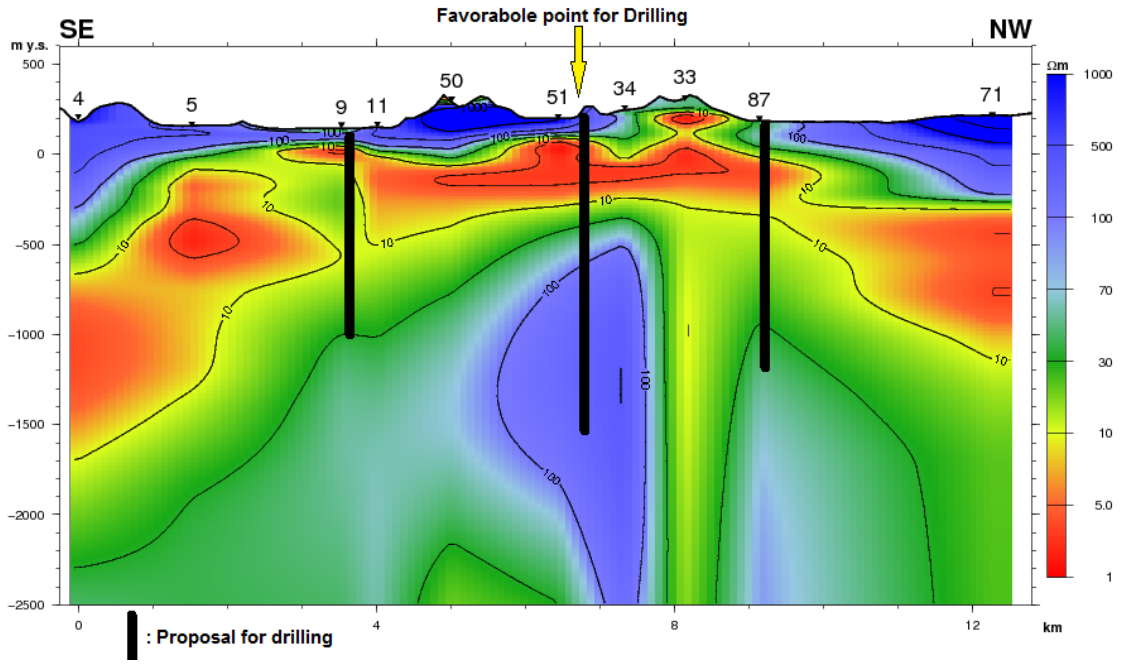

FIGURE 19: Resistivity cross-section from the joint 1-D inversion of TEM and MT extending to 2.5 km b.s.l. with proposed drill sites

6. CONCLUSIONS

From 1-D joint inversion of TEM and MT data, the resistivity cross-sections of the SE-NW profile presented here show, in general, three major resistivity structures:

- Between 320 and 0 m a.s.l. high resistivity (>100 Ωm), associated with surface layers is dominant and can be interpreted as unaltered basaltic lavas and hyaloclastites;
- Between 0 and 600/1000 m b.s.l. a low-resistivity layer (≤ 10 Ωm) is found, which can be correlated with the smectite-zeolite or mixed layer clay alteration zones, indicating temperatures up to about 220°C;
- Below the conductive layer, high resistivity (> 10 Ωm) is observed, which can be correlated with the chlorite-epidote alteration zone as confirmed from the alteration zones of well KR-08 to a depth of about 933 m (Hersir et al., 2010). This indicates the presence of higher temperatures about or above 240-250°C.

The centre of the geothermal reservoir seems to be localised between MT soundings 51 and 34, at levels below 400 m b.s.l.

The drillhole KR-08 confirms high temperatures of 190°C at 400 m depth. The temperature indicated by alteration is higher than the actual measured temperature in the well. This shows that the system has most likely been cooling down (Árnason et al., 2000; Árnason et al., 2010).

Based on the resistivity distribution, three favourable sites are recommended for the realisation of geothermal exploration drilling.

The study was based solely on 1-D joint inversion of a single profile consisting of 10 MT and 10 TEM soundings. A single profile cannot properly determine favourable sites for implementation of geothermal drilling. The resistivity cross-section from the joint 1-D inversion of TEM and MT data of this profile did not reveal a good picture of a conductor at great depths which could be associated to the heat source of the geothermal system. The resistivity cross-section shows a complex resistivity structure at great depth. More resistivity cross-sections are needed to characterise the heat source of the geothermal reservoir in this area.

ACKNOWLEDGEMENTS

This report is submitted to the United Nation University Geothermal Training Programme (UNU-GTP). The research was supervised by Gylfi Páll Hersir, geophysicist at ÍSOR, and Knútur Árnason, Head of Geophysics at ÍSOR. I want to thank them for their guidance, for all their patience, countless hours spent explaining and discussing various problems, and for giving helpful comments.

I am grateful to the Government of Iceland and Dr. Ingvar B. Fridleifsson, Director of the UNU-GTP and Deputy Director, Mr. Lúdvík S. Georgsson, for the UNU-GTP Fellowship. Many thanks go, in particular, to all the other UNU Fellows for valuable discussions on various disciplines of geothermal exploration and for their friendship. I am grateful to the UNU-GTP staff, Ms. Thórhildur Ísberg, Ms. Dorthe H. Holm, Mr. Markús A.G. Wilde and Mr. Ingimar G. Haraldsson for their continuous help during my stay in Iceland.

I wish to express my sincere gratitude to the Vice Presidency in charge of the Energy Ministry of Comoros.

REFERENCES

Árnason, K., 1989: *Central loop transient electromagnetic sounding over a horizontally layered earth*. Orkustofnun, Reykjavík, report OS-89032/JHD-06, 129 pp.

Árnason, K., 2006: *TEMTD. A program for 1D inversion of central-loop TEM and MT data. A short manual*. ÍSOR, Reykjavík, 16 pp.

Árnason, K., Eysteinsson, H., and Hersir, G.P., 2010: Joint 1D inversion of TEM and MT data in the Hengill area, SW Iceland. *Geothermics, 39*, 13-34.

Árnason, K., Karlsdóttir, R., Eysteinsson, H., Flóvenz, Ó.G., and Gudlaugsson, S.Th., 2000: The resistivity structure of high-temperature geothermal systems in Iceland. *Proceedings of the World Geothermal Congress 2000*, *Kyushu-Tohoku, Japan,* 923-928.

Arnórsson, S., Gudmundsson, G., Sigurmundsson, S.G., Björnsson, A., Gunnlaugsson, E., Gíslason, G., Jónsson, J., Einarsson, P., and Björnsson, S., 1975: *Krýsuvík. A general report on the geothermal exploration.* Orkustofnun, Reykjavík, report OS-JHD-7554 (in Icelandic), 71 pp.

Berdichevsky, M.N., 1999: Marginal notes on magnetotellurics. *Surveys in Geophysics, 20*, 341-375.

Eysteinsson, H., 1999: *Resistivity soundings around Sandfell, Reykjanes peninsula*. Orkustofnun, Reykjavík, report OS-99002 (in Icelandic), 71 pp.

Eysteinsson, H., 2001: *Resistivity soundings around Trölladyngja and Núpshlíðarháls, Reykjanes peninsula.* Orkustofnun, Reykjavík, report OS-2001/038 (in Icelandic), 110 pp.

Hersir, G.P., and Björnsson, A., 1991: *Geophysical exploration for geothermal resources. Principles and applications*. UNU-GTP, Iceland, report 15, 94 pp.

Hersir, G.P., Vilhjálmsson, A.M., Rosenkjær, G.K., Eysteinsson, H., and Karlsdóttir, R., 2010: *The Krýsuvík geothermal field. Resistivity soundings 2007 and 2008.* ÍSOR - Iceland GeoSurvey, Reykjavík, report ÍSOR-2010/025 (in Icelandic), 263 pp.

Pellerin, L., and Hohmann, G.W., 1990: Transient electromagnetic inversion: A remedy for magnetotelluric static shifts. *Geophysics, 55-9,* 1242-1250.

Phoenix Geophysics, 2009: *V5 system 2000 MTU/MTU - a user's guide*. Phoenix Geophysics, 19, 190 pp.

Swift Jr., C.M., 1967: *A magnetotelluric investigation of an electrical conductivity anomaly in the southwestern United States.* Massachusetts Institute of Technology, PhD thesis, MA, USA.

Vozoff, K., 1991: The magnetotelluric method. In: Nabighian, M.N (ed), *Electromagnetic methods. Applied Geophysics*, *2*, 641-711.

APPENDIX 1: TEM and MT soundings that were jointly 1-D inverted, data and interpretation

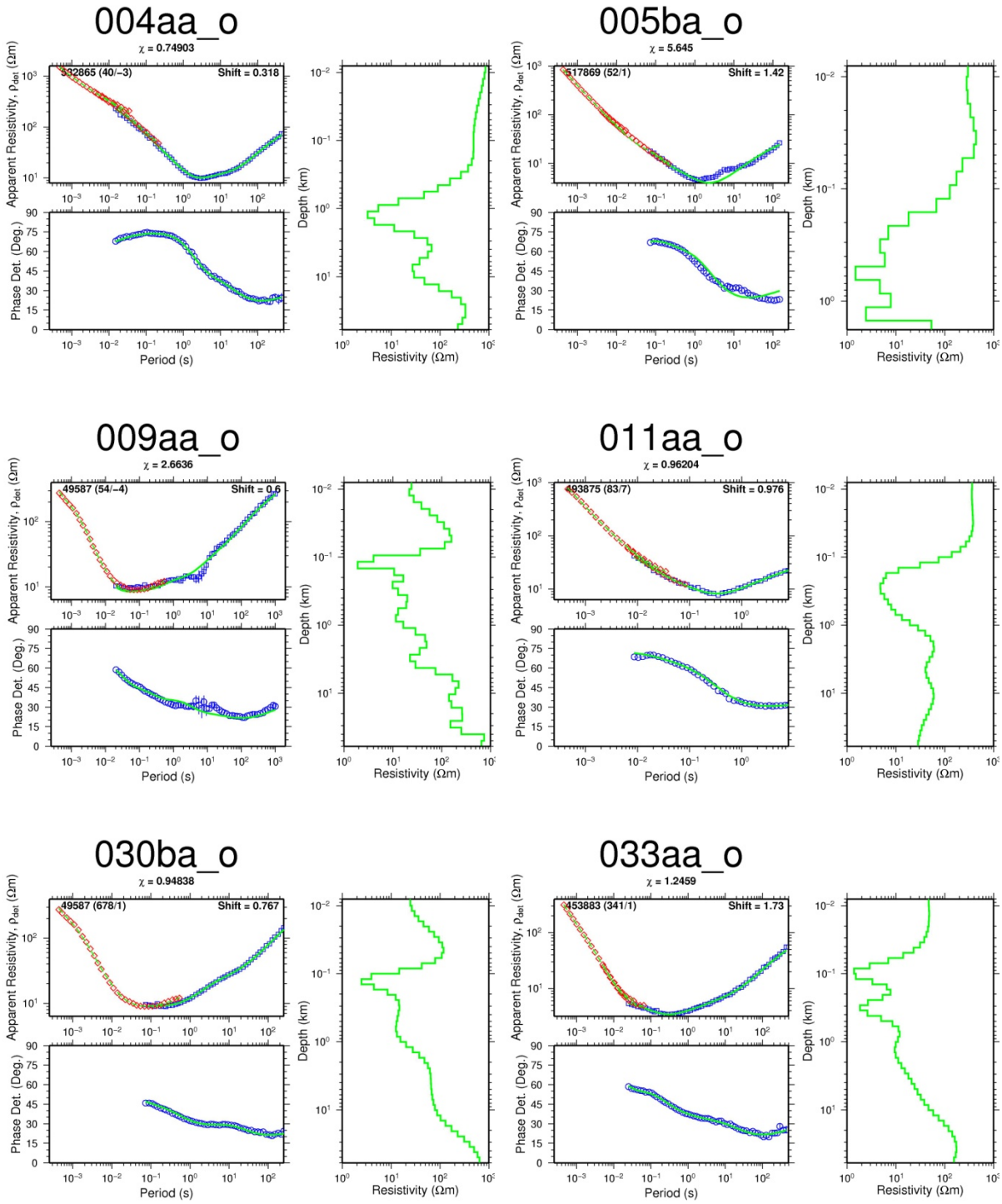

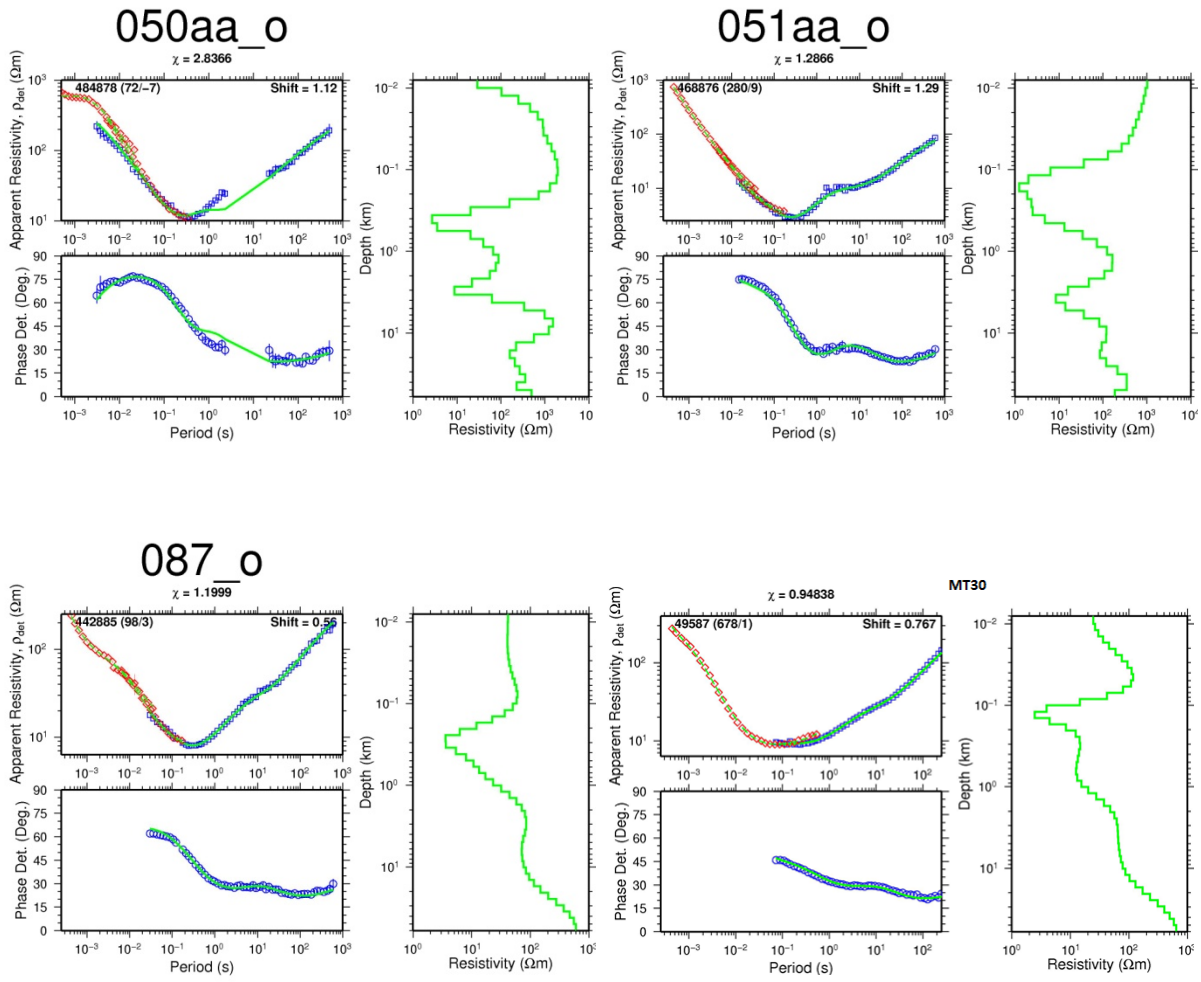
050aa_o
χ = 2.8366
484878 (72/−7)
Shift = 1.12
Apparent Resistivity, ρdet (Ωm)
Phase Det. (Deg.)
Period (s)
Depth (km)
Resistivity (Ωm)
051aa_o
χ = 1.2866
468876 (280/9)
Shift = 1.29
087_o
χ = 1.1999
442885 (98/3)
Shift = 0.55
χ = 0.94838
49587 (678/1)
Shift = 0.767
MT30